Synthesis, Single Crystal Structure and Ionic Conductivity of $Na_{1.96}Ca_{0.96}Eu_{0.04}P_2O_7$

Randal L. Hallford
Department of Chemistry, Midwestern State University, Wichita Falls, TX 76308-2099, USA

Jamal Bennazha
Laboratoire Matériaux Catalyse et Environnement (LMCE), Département de Chimie, Faculté des Sciences et Techniques, Université Hassan II, BP 146, Mohammadia 20650, Morocco

Aicha El Maadi
Laboratoire de Physico-Chimie des Matériaux, Département de Chimie, Faculté des Sciences, Université Ibn Tofail, Kénitra, Morocco

Mohomad El Omari
Equipe Physico-Chimie des Matériaux Condensés, Faculté des Sciences, Université Mou-layIsmaïl BP 4010 Beni M'hamed Meknès Marocco

Ali Boukhari
Laboratoire de Chimie du Solide Appliquée, Département de Chimie, Faculté des Sciences, Université Mohammed V, Avenue Ibn Batouta, Rabat,BP 1014, Morocco

The diphosphate $Na_{1.96}Ca_{0.96}Eu_{0.04}P_2O_7$ has been prepared in powder and single crystal states. The space group is $P\bar{1}$ (Z=2) and the unit cell parameters are: a=5.473(3) Å, b=7.163(4) Å, c=8.897(5) Å, α=69.54(2)°, β=89.12(3)°, γ=88.83(4)°, V=326.7(3) Å^3, Dcalc=2.676 mg/m^3. The refinement converged to R/Rw= 4.08/10.63 for 1876 observed reflections ($I > 2\sigma(I)$). The structure is isotypic to that of $Na_2CaP_2O_7$ and it is characterized by tunnels where Na^+ ions are located. The transport properties of $Na_{1.96}Ca_{0.96}Eu_{0.04}P_2O_7$ are reported.

INTRODUCTION

Recently, the synthesis, single crystal structure, and conductivity of the diphosphates $K_2PdP_2O_7$ and $K_{3.5}Pd_{2.25}(P_2O_7)_2$ were reported [1].

This report is the result of an extension of the work on mixed diphosphates containing both alkaline and transition metal cations. The structure of $Na_2CaP_2O_7$ has been previously determined [2], and the purpose of this work is to create positive vacancies in this matrix in order to produce good electrical performance. The matrix was doped with a trivalent element (Eu^{3+}) producing vacancies in the mobile lattice of sodium cations. The synthesis, crystal structure and the conductivity of $Na_{1.96}Ca_{0.96}Eu_{0.04}P_2O_7$ are herein reported.

2. Experimental

2.1 Synthesis

2.1.1 Powder state synthesis

The starting materials Na_2CO_3, $CaCO_3$, Eu_2O_3 and $(NH_4)_2HPO_4$ of high purity grade (>99%) were heated together in a porcelain crucible to 953 K and then cooled while grinding in an agate mortar until a temperature of 423 K was reached. The reaction occurs according to the following equation:

$$(1-x/2)Na_2CO_3 + (1-x)\,CaCO_3 + x/2\,Eu_2O_3 + 2(NH_4)_2HPO_4 \rightarrow Na_{2-x}Ca_{1-x}Eu_xP_2O_7 + 4NH_3\uparrow + 3H_2O\uparrow + (2-3x/2)CO_2\uparrow$$

(with x= 0.04)

The purity of the final product was evaluated by powder X-ray diffraction using a D500 X-ray diffractometer. A comparison was made with a powder pattern generated from single crystal data of the crystals with the same composition, or by isotipy with the pattern of the isomorphous diphosphate $Na_2CaP_2O_7$ [2].

2.1.2 Single crystal synthesis

The crystals of $Na_{1.96}Ca_{0.96}Eu_{0.04}P_2O_7$ were prepared from the powder obtained at 953 K as described above by a direct fusion method in a porcelain crucible. The melting temperature (1223 K) was maintained for 24 hours and followed by controlled cooling (5°/h) to 773 K, whereupon heating was stopped and allowed to equilibrate at room temperature. The crystals obtained were observed under a polarization microscope as colorless transparent needles.

2.2 Single crystal X-ray diffraction

A single crystal of $Na_{1.96}Ca_{0.96}Eu_{0.04}P_2O_7$ (0.2 x 0.2 x 0.2 mm^3) was mounted on a Siemens P4 automated diffractometer, equipped with graphite monochromated Mo Kα radiation (λ= 0.71073 Å). Data was collected at room temperature with a θ-2θ data collection mode [3]. Three standard reflections were remeasured after each 97 data. The intensities of these reflections showed insignificant variation. Data were corrected for Lorentz, polarization, background, centering and absorption effects. Atomic positional parameters were determined using direct methods [4] and refinements were carried out using full-matrix least-squares techniques [5]. Details of data collection and crystal structure are presented in Table 1.

2.3 Ionic conductivity

The conductivity measurements of $Na_{1.96}Ca_{0.96}Eu_{0.04}P_2O_7$ were carried out on a powdered sample, pressed to a cylindrical pellet form (of thickness = 1.26 mm and diameter = 8.20 mm), and sintered under the same operating conditions as for powder synthesis (973 K for 24 hours). Compactness is approximately 90%. Vacuum evaporated gold was used as the electrode material. The Au//Sample//Au device was placed in a quartz measurement cell, degassed at

Table 1: Crystal data for $Na_{1.96}Ca_{0.96}Eu_{0.04}P_2O_7$.

Formula	$Na_{1.96}Ca_{0.96}Eu_{0.04}P_2O_7$
MW (g/mol)	263.26
Temperature (K)	293(2)
a(Å)	5.473(3)
b(Å)	7.163(4)
c(Å)	8.897(5)
α(°) 69.54(2)	
β(°) 89.12(3)	
γ(°) 88.83(4)	
Volume ($Å^3$)	326.7(3)
Z 2	
Crystal system, Space group	Triclinic, $P\bar{1}$
F(000)	258
Absorption coefficient $\mu MoK_\alpha (mm^{-1})$	1.887
Octants measured	$-7<h<1, -9<k<9, -12<l<12$
Wavelength (Å)	0.71073
Dcal (mg/m^3)	2.676
Independent reflections(R_{int})	2412 (0.0962)
Observed reflections	1876
R/Rw ($I > 2\sigma(I)$)	4.08/10.63

473 K for 2 hours in order to eliminate possible traces of water, then heated to several measurement temperatures.

The electrical properties were determined by a complex impedance method using a frequency response analyzer (Solartron 1260) [6]. The frequency range was $10^{-2} – 10^{6}$ Hz over the thermal interval 300-718 K in several cycles. The real and imaginary parts of the complex impedance ($Z^* = Z'-jZ''$, with $j^2=-1$) were measured as a function of the frequency. The relative resistance of the sample at each temperature was determined as the intersection of the semicircle (extrapolated) of the impedance curve (real component) with the Z′ axis.

RESULTS AND DISCUSSION

3.1 Structure

Figure 1 gives a projection view of the structure of $Na_{1.96}Ca_{0.96}Eu_{0.04}P_2O_7$. The structure is characterized by the presence of two types of tunnels, both parallel to [100] direction. These tunnels are built up from $P_2O_7^{4-}$ moieties and calcium polyhedra. Positional parameters for $Na_{1.96}Ca_{0.96}Eu_{0.04}P_2O_7$ are presented in Table 2. The $P_2O_7^{4-}$ groups presented P-O distances averaging 1.525(3) Å. They are located in staggered conformation with a torsion angle O-P…P-O of 43.4° and a bridge angle P-O-P of 125.49(12)°.

Ca^{2+} cations are surrounded by six oxygen atoms belonging to six different $P_2O_7^{4-}$ groups. The (Ca/Eu)-O distances average 2.362 Å.

The Na atoms are seven-coordinate and are located in two different crystallographic sites: Na(1) and Na(2). The average Na-O distances are 2.598(3) Å for Na(1) and

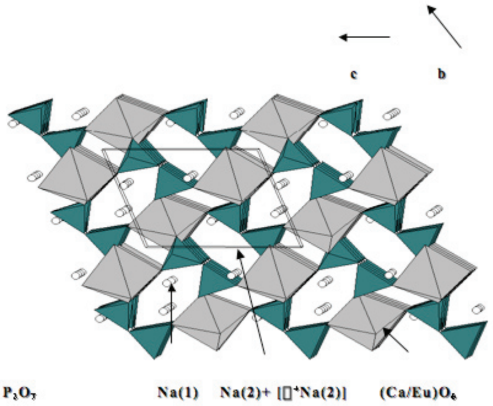

Figure 1: Projection view of $Na_{1.96}Ca_{0.96}Eu_{0.04}P_2O_7$

Table 2: Positional parameters for $Na_{1.96}Ca_{0.96}Eu_{0.04}P_2O_7$

Atom	occupation	x(σ(x))	y(σ(y))	z(σ(z))	Ueq
Ca	0.9633	0.2340(1)	0.2438(1)	0.7233(2)	0.014(1)
Eu	0.0366	0.2340(1)	0.2438(1)	0.7233(2)	0.014(1)
Na(1)	1	0.2332(2)	-0.1391(2)	0.5475(2)	0.023(1)
Na(2)	0.9633+0.04 $^{+}$Na	0.2641(3)	0.7840(3)	0.9812(2)	0.037(1)
P(1)	1	0.2478(1)	0.1170(1)	1.1751(1)	0.011(1)
O(11)	1	0.2745(4)	0.1276(3)	1.0021(2)	0.023(1)
O(12)	1	0.4591(4)	0.0050(3)	1.2822(3)	0.018(1)
O(13)	1	-0.0058(4)	0.0505(3)	1.2466(3)	0.017(1)
O(14)	1	0.2697(4)	0.3507(3)	1.1590(2)	0.016(1)
P(2)	1	0.2951(1)	0.4319(1)	1.3095(1)	0.012(1)
O(21)	1	0.1762(4)	0.2768(3)	1.4554(2)	0.020(1)
O(22)	1	0.1613(4)	0.6335(4)	1.2485(3)	0.022(1)
O(23)	1	0.5706(4)	0.4516(3)	1.3290(3)	0.023(1)

Ueq : Equivalent isotropic U defined as one third of the trace of the orthogonalized Vij tensor.

2.658(3) Å for Na(2). The substitution of Ca^{2+} by Eu^{3+} cations in $Na_{1.96}Ca_{0.96}Eu_{0.04}P_2O_7$ generated positive vacancies in the sub lattice of Na(2), ($^{+}$Na(2)) which should favor the transport properties of the diphosphate.

The structure of the diphosphate $Na_{1.96}Ca_{0.96}Eu_{0.04}P_2O_7$ is isomorphous to that of $Na_2CaP_2O_7$, previously determined [2]. It is very similar to those of the diphosphates $K_2SrP_2O_7$ [7], $K_2CdP_2O_7$ [8] and $K_2MnP_2O_7$ [9].

3.2 Conductivity

Complex impedance diagrams of Z″(kΩ) as a function of Z′(kΩ), are presented in Figure 2 for $Na_{1.96}Ca_{0.96}Eu_{0.04}P_2O_7$ at 623,

Table 3: Selected bond distances (Å) and angles (°) for $Na_{1.96}Ca_{0.96}Eu_{0.04}P_2O_7$

Ca/Eu-O(11)	2.336(3)	O(11)-Ca/Eu-O(21′)	165.61(8)
Ca/Eu-O(12^{v})	2.436(2)	O(11)-Ca/Eu-O(23″)	97.24(9)
Ca/Eu-O(13^{iv})	2.361(3)	O(21′)-Ca/Eu-O(23″)	96.44(9)
Ca/Eu-O(21′)	2.337(3)	O(11)-Ca/Eu-O(22‴)	89.46(9)
Ca/Eu-O(22‴)	2.361(3)	O(21′)-Ca/Eu-O(22‴)	93.68(9)
Ca/Eu-O(23″)	2.343(2)	O(23‴)-Ca/Eu-O(22‴)	95.42(9)
		O(11)-Ca/Eu-O(13^{iv})	87.81(8)
		O(21′)-Ca/Eu-O(13^{iv})	78.82(8)
Na(1)-O(12′)	2.534(3)	O(23″)-Ca/Eu-O(13^{iv})	173.91(8)
Na(1)-O12^{v})	2.687(3)	O(22‴)-Ca/Eu-O(13^{iv})	81.17(9)
Na(1)-O(13^{iv})	2.453(3)	O(11)-Ca/Eu-O(12^{v})	87.57(8)
Na(1)-O(21 ^{iv})	2.471(3)	O(21′)-Ca/Eu-O(12^{v})	83.92(8)
Na(1)-O(21′)	2.812(3)	O(23″)-Ca/Eu-O(12^{v})	108.31(9)
Na(1)-O(13′)	2.866(3)	O(22‴)-Ca/Eu-O(12^{v})	156.27(8)
Na(1)-O(23^{v})	2.365(3)	O(13^{iv})-Ca/Eu-O(12^{v})	108.1(1)
Na(2)-O(14)	2.950(3)		
Na(2)-O(22)	2.308(3)	O(11)-P(1)-O(12)	113.35(13)
Na(2)-O(11^{vi})	2.528(3)	O(12)-P(1)-O(13)	113.90(13)
Na(2)O(11″)	2.637(3)	O(12)-P(1)-O(14)	106.34(12)
Na(2)-O(11‴)	3.016(3)	O(11)-P(1)-O(13)	113.06(13)
Na(2)-O(12″)	2.753(3)	O(11)-P(1)-O(14)	102.72(12)
Na(2)-O(13‴)	2.419(3)	O(13)-P(1)-O(14)	106.30(12)
P(1)-O(11)	1.521(2)	O(14)-P(2)-O(21)	106.75(12)
P(1)-O(12)	1.533(2)	O(14)-P(2)-O(22)	102.79(13)
P(1)-O(13)	1.532(2)	O(21)-P(2)-O(22)	114.74(14)
P(1)-O(14)	1.637(2)	O(14)-P(2)-O(23)	105.49(13)
		O(22)-P(2)-O(23)	112.70(13)
		O(21)-P(2)-O(23)	113.17(13)
P(2)-O(14)	1.644(2)		
P(2)-O(21)	1.529 (2)		
P(2)-O(22)	1.528(2)	P(1)-O(14)-P(2)	125.49(12)
P(2)-O(23)	1.536(2)		

Symmetry codes: ′ = x, y, z-1 ; ″ = -x+1, -y+1, -z+2 ; ‴ = -x, -y+1, -z+2, ^{iv} = -x, -y, -z+2 ; ^{v} = -x+1, -y, -z+2 ; ^{vi} = x, y+1, z

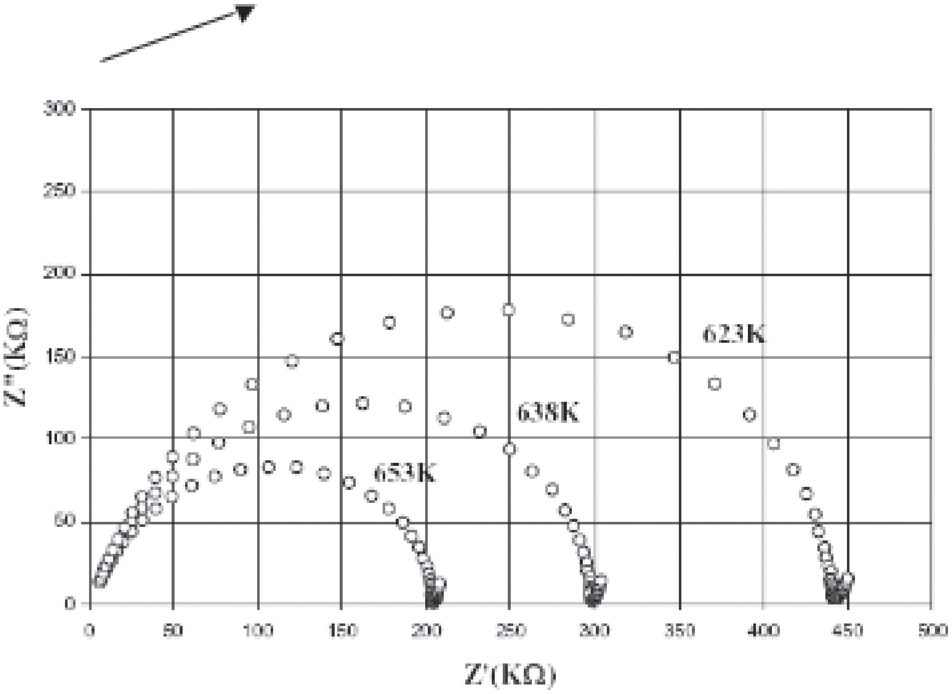

Figure 2: Impedance diagram for $Na_{1.96}Ca_{0.96}Eu_{0.04}P_2O_7$.

638 and 653 K. The electric behavior of this phosphate is a Cole-Cole type [10-11]. The semi-circles represent the bulk response of the sample. The low frequency region of the semi-circle graph shows an inclined spike which indicates a purely ionic conductivity. In fact, this spike represents the polarization phenomena at the electrode-electrolyte interface.

The ionic conductivity is due to the sodium cations which constitute the carriers across the tunnels of the structure. This mobility is expected from the crystallographic data (Table 1) that shows a higher isotropic coefficient for the sodium sites Na(1) and Na(2). This coefficient is more important for Na(2) which have positive vacancies in their respective tunnels.

The temperature dependence of the conductivity is presented in Figure 3 as a plot of Log σT versus 1000/T. There are two distinct domains. The transition between them occurs at 544 K, and each domain is seen as a linear segment which follows the Arrhenius law. The linear fit to $\sigma T = \sigma_0 \exp(-\Delta E_\sigma/kT)$ is shown with correlation coefficients equal to 0.99 for both domains.

Electrical data relative to $Na_{1.96}Ca_{0.96}Eu_{0.04}P_2O_7$ are listed in Table 4. Differential Scanning Calorimetery (DSC) measurements on $Na_{1.96}Ca_{0.96}Eu_{0.04}P_2O_7$ has shown the absence of a thermal (structural) transition in the range of temperature studied by the conductivity, and indicates that the change of conductivity at 544 K can be attributed to the mobile lattice of sodium cations Na(1) and Na(2). Thus, two types of tunnels are present, one with Na(1) and the second with Na(2) + positive vacancies.

The Na(2)+ vacancies are probably responsible for the first domain below 544 K because they are faster ($\Delta E_{L.T.} = 0.71$eV) and the transport is facilitated by the presence of positive vacancies. Na(1) will add their contribution to the next domain over 544 K ($\Delta E_{H.T.} = 0.95$eV).

The electrical performance of $Na_{1.96}Ca_{0.96}Eu_{0.04}P_2O_7$ is comparable to that

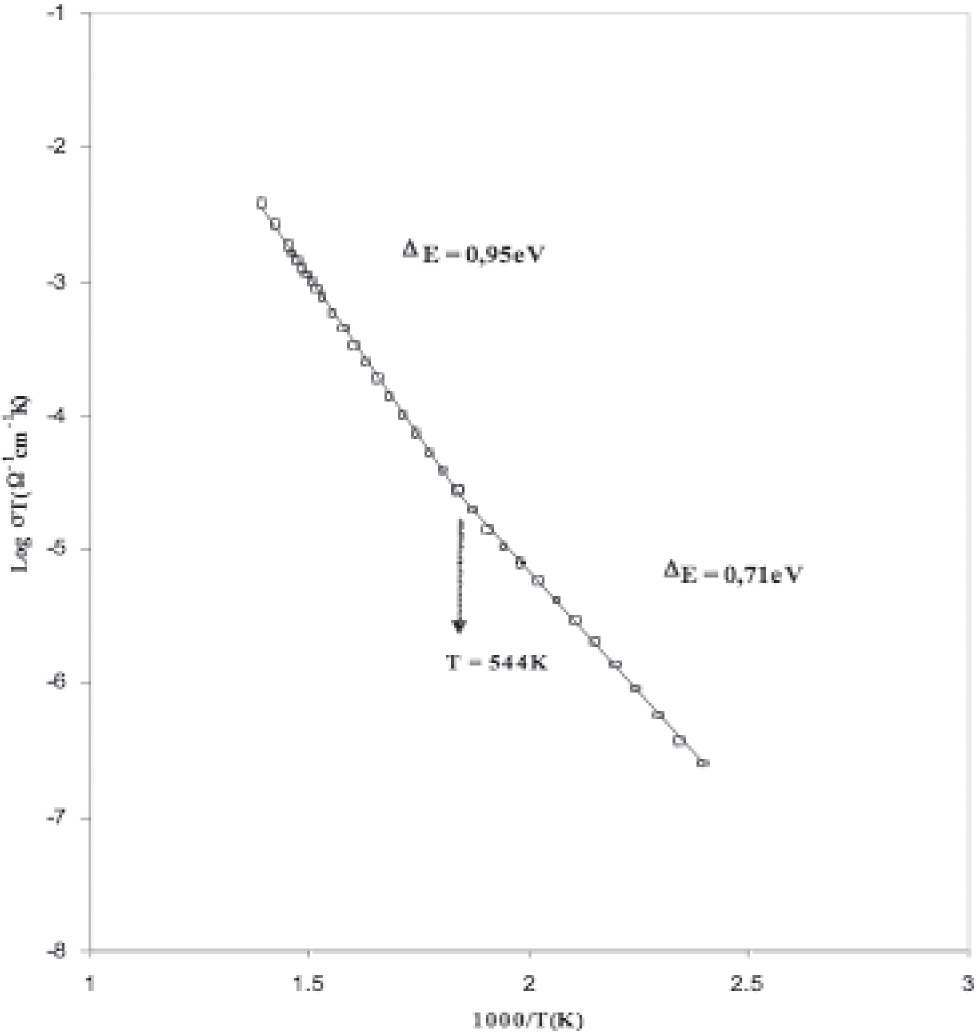

Figure 3: Variation of ionic conductivity as a function of 1000/T for $Na_{1.96}Ca_{0.96}Eu_{0.04}P_2O_7$.

Table 4: Electrical data for $Na_{1.96}Ca_{0.96}Eu_{0.04}P_2O_7$.

$\Delta E_{L.T}$(eV)±0.02	$\Delta E_{H.T}$(eV) ±0.02	$\sigma_{200°C}$($\Omega^{-1}cm^{-1}$) ±0.02	$\sigma_{400°C}$($\Omega^{-1}cm^{-1}$)±0.02	Log $\sigma_{0\ (L.T)}$	Log $\sigma_{0\ (H.T)}$
0.71	0.95	6.13 10^{-9}	1.88 10^{-6}	2.07	4.25

found in other diphosphates in the literature. For example, $Na_2CoP_2O_7$, [12] with a structure characterized by tunnels where sodium cations are located, has $\sigma_{400°C}$= 2. 10^{-5} $\Omega^{-1}cm^{-1}$ with an activation energy of 0.63 eV. $Na_2PbP_2O_7$, [13] with structure characterized by sodium cations carriers belonging to the space between layers, has $\sigma_{400°C}$= 9.4 10^{-5} $\Omega^{-1}cm^{-1}$ and an activation energy of 0.9 eV. The conductivity of $Ca_2P_2O_7$-$Na_4P_2O_7$ [14] has been studied and the best results were $\sigma_{300°C}$= 2. 10^{-6} $\Omega^{-1}cm^{-1}$ obtained for 95% $Na_4P_2O_7$.

CONCLUSION

Synthesis of both powder state and single crystals of the diphosphate $Na_{1.96}Ca_{0.96}Eu_{0.04}P_2O_7$ are reported.

The structure has the triclinic symmetry with the space group $P\bar{1}$ (Z=2) and the unit cell parameters are: a=5.473(3) Å, b=7.163(4) Å, c=8.897(5) Å, α=69.54(2)°, β=89.12(3)°, γ=88.83(4)°, V=326.7(3) $Å^3$, and Dcalc=2.676 mg/m^3. The refinements converged to R/Rw= 4.08/10.63. The structure is isotypic to that of $Na_2CaP_2O_7$ and it is characterized by tunnels where Na^+ ions are located.

Electrical properties of $Na_{1.96}Ca_{0.96}Eu_{0.04}P_2O_7$ have been determined by impedance spectroscopy. This material shows a pure ionic conductivity due to the Na+ carriers that are mobile in the tunnels along the a-axis. The material offers suitable tunnel dimensions permitting the electrical conduction properties associated with the presence of the Na^+ ions.

5. ACKNOWLEDGMENTS

Randal Hallford gratefully acknowledges financial support by The Welch Foundation, Grant # AO-0001, for the computer hardware and software for computational crystallography. The author is also grateful to Midwestern State University and the College of Science and Mathematics for support in the form of laboratory space, partial funding and salary.

REFERENCES

[1] A. Elmaadi, J. Bennazha, J. M. Réau, A. Boukhari and E. M. Holt, Materials Research Bulletin 38 (2003) 865-874.

[2] J. Bennazha, A. Boukhari and E.M.Holt , Solid State Sciences, t.1, (1999), 373-380

[3] XSCANS: XSCANS Users Manual, Siemens Analytical X-ray Instruments, Inc., Madison, WI, USA, (1991)

[4] SHELXS: GM. Sheldrick, SHELXS-97, Acta Crystallogr. A46 (1990) 467-473

[5] SHELXL: GM. Sheldrick, SHELXL-98 A program for the refinement of Crystal Structures from diffraction Data, University of Gottingen, (1998)

[6] J. F. Bauerle, J. Phys. Chem. Solids 30 (1969) 2657-2670.

[7] V. K. Trunov, Yu. V. Ooznenko, S.P. Sirotinkin and N. B. Tskhelashvili, Neorg. Mater., 27(9) (1991) 2370-2371.

[8] R. Faggiani and C. Calvo , Can. J. Chem., 54 (1976) 3319-3324.

[9] A. Elmaadi, A. Boukhari, E. M. Holt and S. Flandrois, C. R. Acad. Sci. Paris, t 318, Serie II (1994) 765-770.

[10] K. S. Cole and R. H. Cole, J. Chem. Phys., 9 (1941) 341-351,

[11] D. P. Almond, A.R. West, Solid State Ionics 11 (1983) 57-64.

[12] F. Sanz, C. Parada, J. M. Rojo, C. Ruiz-Valero and R. Saez-Puche, Journal of Solid State Chemistry, 145, (1999) 604-611

[13] N. Dridi, A. Boukhari, J. M. Réau, E. Arbib and E. M. Holt, Solid State Ionics 127 (2000) 141-149

[14] V. Vincent, G. Nihoul and J. R. Gavarri, Solid State Ionics, 92, (1996) 11

Received: April 25, 2008; AcceptedDecember 8, 2008.